

Numerical solution of electromagnetic problem in horizontal porous medium

Alaa A. Hammodat*

*Department of Mathematics
College of Education for Pure Science
University of Mosul
Mosul
Iraq
alaahammadat@uomosul.edu.iq*

Hamsa D. Saleem

*Department of Mathematics
College of Education for Pure Science
University of Mosul
Mosul
Iraq
hamsa_dawood@uomosul.edu.iq*

Abstract. A model of heat transfer in a channel of porous walls under the influence of a vertical electromotive force (EMF) with natural convection and thermal radiation of a dissipative fluid is discussed in the channel plane. Using the finite difference method, the partial differential equations that govern the issue have been formulated and solved. Where, using successive iterations of the above method on the equations that are in the time-dependent form, we were able to reach the required solution to the problem. Besides, the temperature distribution behaviour inside the channel was noticed, and the effect of the thermal behaviour of Rayleigh number, Brinkman number, Prandtl number, Eckert number and Hartmann number was also studied. By creating a computer program using MATLAB, we solved the system.

Keywords: transfer of heat, porous medium, Brinkman number, Eckert number, Hartmann number, Prandtl number.

1. Introduction

The study of fluid flow in a porous wall channel is very interesting since it has a wide range of implementation, and this is because these flows have many engineering and geophysical applications that include geothermal resources, blood flow inside human bodies, building insulation, oil extraction, heat salt leaching in soils, lymph transport flow system, urinary circulatory system [1]. A analysis of some previous work in this field is provided below.

In enclosures with localized heating natural convection was studied from below the creeping flow to the onset of laminar instability (see [2]).

*. Corresponding author

The convection in a rotating cylindrical annulus under the influence of its symbol MF only mention in [3]. They examined the effect MFs radial and azimuthal components on the convection columns in the fluid-filled gap between two cylinders rotating stiffly numerical around their shared vertical axis, cooling the inner cylinder, heating the outer one so that the centrifugal force provides the buoyancy force driving the convection.

The effects of radiative in magneto fluid-dynamic channel flow demonstrate ref. [4], he has expanded plane Hartmann flow to account for thermally radiative effects with variable absorption coefficient and non-uniform temperature of channel walls. In addition, several dimensions of stability have been reviewed.

While uses a 2-dimensional Galerkin formulation of the 3-dimensional Oberbeck-Boussinesq equations to evaluate the convection beginning in an infinite rigid horizontal channel that has a uniformly lower heat source [5]. In order to include convection patterns, they expanded the previous findings to higher truncation levels.

In a fluid layer with a lower heat source, the thermal convection issue is introduced [6] and numerically resolved when the layer has high vertical MF parameters. The stability of 2-dimensional convection rolls is studied by using various values of the Hartmann number within the area (200-400).

The convection inside a rotating cylindrical annulus, by a system that contains three coupled amplitude equations, is investigated [7]. They described many features to a good approximation, and show that the time integrations based on the Galerkin expansion display transitions to chaotic convection at a high number of Rayleigh.

The fully defined free convection problem of two fluid magneto hydrodynamic (MHD) flow in a slanted channel is addressed, its observed that the flow can be effectively dominated by adequate adjustment of the values for the heights, electrical conductivity, and viscosity ratios of two fluids [8].

In [9] studied linear stability to obtain the numerical solution of a multi-layer system consisting of the onset of finger convection in a fluid layer overlying a porous layer using the spectral Chebyshev polynomial process.

In [10] the investigation of combined effects of a transverse magnetic field and irradiative heat transfer on the unsteady flow of a conducting optically thin fluid through a channel filled with the saturated porous medium the temperature of a non-uniform wall, his results showed that increasing magnetic field intensity reduce wall shear stress while increasing radiation parameter through heat absorption causes an increase in the magnetic of wall shear stress.

In [11] proposed a solution to the magneto hydrodynamic(MHD) problem analytically free convection flow of an electrically conducting fluid between two heated parallel plates in the existence of an induced MF. It has been noted that the skin-friction increases first then gradually decreases with the increase of Hartmann number at $y=1$.

The impacts of radiation on (MHD) flow of Maxwell fluid in a channel with a porous medium by employing the homotopy analysis method (HAM) discussed [12].

In [13] investigated the 2-dimensional steady flow of electrically conducting incompressible power-law fluid past an infinite porous flat plate subjected to suction or blowing, they are also analyzed the heat transfer flow in the case when the plate is held at a fixed temperature. In the same year, the homotopy analysis method (HAM) is applied to obtain the analytic solution of partial differential equations. Numerical results and graphical representation strongly reconfirm the efficiency of the proposed scheme [14].

In [15] addressed the stability analysis in the glass cavity, and this analysis was achieved by finding the self-values for the system that could or could not be determined by the growth of the disturbance after making linear equations.

In [16] Studied the approximated solutions for heat transfer over a porous plate and steady MHD mixed convection boundary layer flow in the existence of the thermal and velocity stumble, they found the MF impact on a viscous incompressible fluid increase the fluid velocity by reducing the drag on the flow that causes a decrease in the temperature fluid.

In [17] Presented the mass transfer impact, viscous suction parameter, and dissipative on the 2-dimensional steady hydro magnetic viscous fluid flow between two parallel plates in the presence of thermal radiation and we find that velocity, temperature, and concentration decrease with the increase of variable suction parameter and Reynolds number as well as the relation between the different quality physicals.

In [18] Presented a Crank-Nicolson finite difference method to solve the time-fractional 2-dimensional sub-diffusion equation in the case where the Grunwald-Letnikov definition is used for the time-fractional derivative. The stability and convergence of the proposed Crank-Nicolson scheme are also analyzed as well as the numerical examples are presented to test that the numerical scheme is accurate and feasible. In the same year, The modified implicit finite difference approximation of the stability and convergence of the proposed scheme is analyzed [19]. Its founded that show that the scheme is unconditionally stable and the approximate solution converges to the exact solution.

Numerical Solution the motion, heat transfer, and diffusion of the equation in the Porous medium with the presence of Radiation and magnetic field (MF) was studied [20]. It has been found that the parameters have a major effect on the Solution of these Equations. The goal of this research is to study the flow of fluids in a cross-section under the influence of the electromagnetic field (EMF) and to solve the partial differential equations that regulate the problem using the method of (ADI). In addition to showing the behaviour of temperatures inside the cross-section and the effect of physical quantities.

2. Statement of issue

After applying a continuous (EMF) to the fluid, we can research the flow of an electrically conductive fluid inside a segment of a horizontal channel so that the fluid transforms into a magnetized fluid. Assume that the temperature of the horizontal and vertical walls is expressed by τ_c, τ_h and $\tau_h > \tau_c$. The distance between the lower and upper walls is expressed by H and the cross-section length is represented by L . The y - axis is defined by reprinted vertical projected electromagnetic field (EMF) and a magnetic fluid(MF) is created after the electromagnetic field (EMF) is shed that flows to the x - axis and an (EMF) is produced in the direction of the z - axis that is small enough to be ignored as shown in Figure 1:

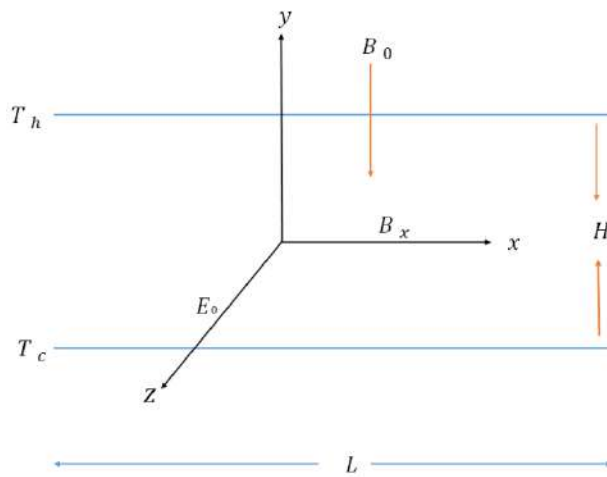


Figure 1: Physical Model and System of Coordinates.

$$(1) \quad \frac{\partial v}{\partial x} + \frac{\partial v}{\partial y} = 0,$$

$$(2) \quad \frac{\partial u}{\partial t} + v \frac{\partial v}{\partial x} + \nu \frac{\partial v}{\partial y} = -\frac{1}{\rho} \frac{\partial p}{\partial x} + \frac{\mu}{\rho} \nabla^2 v + \frac{\sigma E_0 \beta_0}{\rho} + \frac{\sigma E_0 \beta_0 v}{\rho} - \frac{\sigma \beta_x \beta_0 \nu}{\rho},$$

$$(3) \quad \frac{\partial v}{\partial t} + v \frac{\partial v}{\partial x} + \nu \frac{\partial v}{\partial y} = -\frac{1}{\rho} \frac{\partial p}{\partial y} + \frac{\mu}{\rho} \nabla^2 v - \frac{\sigma E_0 \beta_x}{\rho} - \frac{\sigma \beta_x \beta_0 v}{\rho} + \frac{\sigma \beta_x^2 \nu}{\rho} - g\beta [\tau - \tau_c],$$

$$(4) \quad \frac{\partial \tau}{\partial t} + v \frac{\partial \tau}{\partial x} + \nu \frac{\partial \tau}{\partial y}$$

$$= \alpha \nabla^2 \tau + \frac{1}{\rho C_p} \left[\frac{\partial q_x}{\partial x} + \frac{\partial q_y}{\partial y} \right] + \frac{\mu}{\rho C_p} \left[\left[\frac{\partial v}{\partial x} \right]^2 + \left[\frac{\partial v}{\partial y} \right]^2 \right].$$

We differentiate the equation (2) for y and the equation (3) for x in order to get the general motion equation, and then subtract the two equations, we get:

$$(5) \quad \frac{\partial}{\partial t} \left[\frac{\partial v}{\partial x} - \frac{\partial v}{\partial y} \right] + \left[\frac{\partial}{\partial x} \left[v \frac{\partial v}{\partial x} + \nu \frac{\partial v}{\partial y} \right] - \frac{\partial}{\partial y} \left[v \frac{\partial v}{\partial x} + \nu \frac{\partial v}{\partial y} \right] \right] \\ = \frac{\mu}{\rho} \nabla^2 \left[\frac{\partial v}{\partial x} - \frac{\partial v}{\partial y} \right] - g\beta \frac{\partial \tau}{\partial x} + \frac{\sigma \beta_x \beta_0}{\rho} \left[\frac{\partial v}{\partial y} - \frac{\partial v}{\partial x} \right] + \frac{\sigma \beta_x^2}{\rho} \frac{\partial v}{\partial x} - \frac{\sigma E_0 \beta_0}{\rho} \frac{\partial v}{\partial y},$$

where v, ν are the velocity components in x, y respectively, t is the time and $\tau, P, \rho, \sigma, E_0, \beta_0, \beta_x, \mu, g, \beta, C_p, \alpha, q_x, q_y$ temperature, pressure, density, kinematic viscosity, Electric field vector, The magnetic field vector is in the direction of x and y , viscosity, gravitational acceleration, thermal expansion coefficient, specific heat at constant pressure, thermal diffusivity, radiation components in x, y respectively. With the boundary conditions below:

$$(6) \quad \begin{aligned} \tau [x, (y = 0, H)] &= \tau_c, \tau_h, \\ \frac{\partial \tau}{\partial x} &= 0, x = 0, L \\ v [(x = 0, L), y] &= \nu [(x = 0, L), y] = 0, \\ v [x, (y = 0, H)] &= \nu [x, (y = 0, H)] = 0. \end{aligned}$$

3. Non-dimensional form

We need to add the following non-dimensional quantities to solve the governing equations (1), (4) and (5) with the boundary conditions (6) [24].

$$(7) \quad \begin{aligned} u &= v_0 v^*, & \nu &= \nu_0 \nu^*, & v_0 &= \sqrt{g\beta \Delta \tau L}, & t &= \frac{L}{v_0} t^*, \\ x &= Lx^*, & y &= Ly^*, & \vartheta &= \frac{\tau - \tau_c}{\tau_h - \tau_c}, & \vec{q} &= \tau_1^4 \sigma \vec{Q}. \end{aligned}$$

When these quantities are substituted into equations (1), (4) and (5), the governing equations become:

$$(8) \quad \frac{\partial v^*}{\partial x^*} + \frac{\partial v^*}{\partial y^*} = 0, \\ (9) \quad \frac{\partial}{\partial t^*} \left(\frac{\partial v^*}{\partial x^*} - \frac{\partial v^*}{\partial y^*} \right) + \frac{\partial}{\partial x^*} \left(v^* \frac{\partial v^*}{\partial x^*} + \nu^* \frac{\partial v^*}{\partial y^*} \right) - \frac{\partial}{\partial y^*} \left(v^* \frac{\partial v^*}{\partial x^*} + \nu^* \frac{\partial v^*}{\partial y^*} \right) \\ = \sqrt{\frac{P_r}{Ra}} \nabla^2 \left(\frac{\partial v^*}{\partial x^*} - \frac{\partial v^*}{\partial y^*} \right) - \frac{\partial \vartheta}{\partial x^*} - (Ha)^2 \sqrt{\frac{P_r}{Ra}} \left(\frac{\partial v^*}{\partial y^*} - \frac{\partial v^*}{\partial x^*} \right) \\ + (Ha)^2 \sqrt{\frac{P_r}{Ra}} \frac{\partial v^*}{\partial x^*} - I(Ha)^2 \sqrt{\frac{P_r}{Ra}} \frac{\partial v^*}{\partial y^*}.$$

But $v^* = \frac{\partial \Psi^*}{\partial y^*}$ and $\nu^* = -\frac{\partial \Psi^*}{\partial x^*}$ stream function [23], then the equation of general motion becomes: $-\frac{\partial}{\partial t^*} \nabla^2 \Psi^* = -\sqrt{\frac{P_r}{R_a}} \nabla^4 \Psi^* - (H_a)^2 \sqrt{\frac{P_r}{R_a}} \nabla^2 \Psi^*$. Put $\varepsilon^* = -\nabla^2 \Psi^*$, and then:

$$(10) \quad \frac{\partial \varepsilon^*}{\partial t^*} = -\sqrt{\frac{P_r}{R_a}} \nabla^2 \varepsilon^* - (H_a)^2 \sqrt{\frac{P_r}{R_a}} \varepsilon^*,$$

$$(11) \quad \frac{\partial \vartheta}{\partial t^*} + v^* \frac{\partial \vartheta}{\partial x^*} + \nu^* \frac{\partial \vartheta}{\partial y^*} = \frac{1}{\sqrt{P_r R_a}} \nabla^2 \vartheta - \frac{F_s \beta_0 R_e}{\sqrt{P_r R_a}} \nabla \vec{Q} + 2 \frac{F_s}{\sqrt{P_r R_a}} \left(\left(\frac{\partial v^*}{\partial x^*} \right)^2 + \left(\frac{\partial \nu^*}{\partial y^*} \right)^2 \right)$$

and that is about it $\nabla \cdot \vec{Q} = 16\omega^* \vartheta - 12\omega^*$ [4], equation (11) then becomes:

$$(12) \quad \frac{\partial \vartheta}{\partial t^*} + v^* \frac{\partial \vartheta}{\partial x^*} + \nu^* \frac{\partial \vartheta}{\partial y^*} = \frac{1}{\sqrt{P_r R_a}} \nabla^2 \vartheta - \frac{F_s \beta_0 R_e}{\sqrt{P_r R_a}} (16\omega^* \vartheta - 12\omega^*) + \phi.$$

Let $\phi = \frac{2F_s}{\sqrt{P_r R_a}} \left(\left(\frac{\partial v^*}{\partial x^*} \right)^2 + \left(\frac{\partial \nu^*}{\partial y^*} \right)^2 \right)$ physical quantities, and $I = \frac{E_0}{\beta_0}$, $E_c = \frac{v^{*2}}{C_p \tau_1}$, $R_a = \frac{\rho g \beta (\tau_h - \tau_c) L^3}{\mu \alpha}$, $R_e = \frac{h \rho v^*}{\mu}$, $\omega^* = \alpha_0 h$, $\beta_0 = \frac{\rho v^{*3}}{\tau_1^4 \sigma}$, $P_r = \frac{\mu C_p}{\kappa}$, $F_s = P_r E_c$, $H_a = \beta_0 L \sqrt{\frac{\sigma}{\mu}}$, are Inductance, Eckert number, Rayleigh number, Reynolds number, Bouger number, Boltzmann number, Prandtl number, Brinkman number, and Hartmann number respectively. The non-dimensional boundary condition becomes:

$$(13) \quad \begin{aligned} \vartheta &= 0, 1.0 && \text{at} && y^* = 0, 1, \\ \frac{\partial \vartheta}{\partial x^*} &= 0 && \text{at} && x^* = 0, 1, \\ v^* &= \nu^* = 0.0 && \text{at} && y^* = 0, 1. \end{aligned}$$

4. Solution process

To solve the system of equations (8), (10) and (12) with the boundary conditions (13), we use the ADI finite difference method [22], and achieve this we have to start with the last equation(12), heat equation and finally equation(10), motion equation as follows:

4.1 Equation of heat

$$(14) \quad \begin{aligned} &\frac{\vartheta_{i,j}^* - \vartheta_{i,j,n}}{\frac{\Delta t}{2}} + v_{i,j,n}^* \frac{\vartheta_{i+1,j}^* - \vartheta_{i-1,j}^*}{2\Delta x^*} + \nu_{i,j,n}^* \frac{\vartheta_{i,j+1,n} - \vartheta_{i,j-1,n}}{2\Delta y^*} \\ &= -\frac{F_s \beta_0 R_e}{\sqrt{P_r R_a}} (16\omega^* \vartheta_{i,j,n} - 12\omega^*) - \frac{1}{\sqrt{P_r R_a}} \left(\frac{\vartheta_{i+1,j}^* - 2\vartheta_{i,j}^* + \vartheta_{i-1,j}^*}{(\Delta x^*)^2} \right. \\ &\quad \left. + \frac{\vartheta_{i,j+1,n} - 2\vartheta_{i,j,n} + \vartheta_{i,j-1,n}}{(\Delta y^*)^2} \right) + \phi, \end{aligned}$$

$$\begin{aligned}
 & \frac{\vartheta_{i,j,n+1} - \vartheta_{i,j}^*}{\frac{\Delta t}{2}} + \nu_{i,j,n}^* \frac{\vartheta_{i+1,j}^* - \vartheta_{i-1,j}^*}{2\Delta x^*} + \nu_{i,j,n}^* \frac{\vartheta_{i,j+1,n+1} - \vartheta_{i,j-1,n+1}}{2\Delta y^*} \\
 (15) \quad & = \frac{1}{\sqrt{P_r R_a}} \left(\frac{\vartheta_{i+1,j}^* - 2\vartheta_{i,j}^* + \vartheta_{i-1,j}^*}{(\Delta x^*)^2} + \frac{\vartheta_{i,j+1,n+1} - 2\vartheta_{i,j,n+1} + \vartheta_{i,j-1,n+1}}{(\Delta y^*)^2} \right) \\
 & - \frac{F_s \beta_0 R_e}{\sqrt{P_r R_a}} (16\omega^* \vartheta_{i,j,n+1} - 12\omega^*) + \phi.
 \end{aligned}$$

Under boundary conditions,

$$(16) \quad \vartheta_{i,0,n} = 0, \vartheta_{i,N,n} = 1.0.$$

Equations (14) and (15) can be reduced in order to give,

$$(17) \quad A_1(i)\vartheta_{i-1,j}^* + B_1(i)\vartheta_{i,j}^* + C_1(i)\vartheta_{i+1,j}^* = D_1(i)$$

where

$$\begin{aligned}
 A_1(i) &= - \left(\frac{1}{\sqrt{P_r R_a}} + \frac{\Delta x^*}{2} \nu_{i,j,n}^* \right), \\
 B_1(i) &= 2 \left(\frac{(\Delta x^*)^2}{\Delta t} + \frac{1}{\sqrt{P_r R_a}} \right) \\
 C_1(i) &= \left(\frac{1}{\sqrt{P_r R_a}} - \frac{\Delta x^*}{2} \nu_{i,j,n}^* \right), \\
 D_1(i) &= \left(\frac{1}{\sqrt{P_r R_a}} + \frac{\Delta y^*}{2} \nu_{i,j,n}^* \right) \vartheta_{i,j-1,n} + \frac{12F_s \beta_0 R_e \omega^* (\Delta x^*)^2}{\sqrt{P_r R_a}} \\
 &+ 2 \left(\frac{(\Delta y^*)^2}{\Delta t} - \frac{1}{\sqrt{P_r R_a}} - \frac{8F_s \beta_0 R_e \omega^* (\Delta y^*)^2}{\sqrt{P_r R_a}} \right) \vartheta_{i,j,n} \\
 &+ \left(\frac{1}{\sqrt{P_r R_a}} - \frac{\Delta y^*}{2} \nu_{i,j,n}^* \right) \vartheta_{i,j+1,n} + (\Delta x^*)^2 \phi.
 \end{aligned}$$

Followed,

$$(18) \quad A_2(i)\vartheta_{i,j-1,n+1} + B_2(i)\vartheta_{i,j,n+1} + C_2(i)\vartheta_{i,j+1,n+1} = D_2(i)$$

where

$$\begin{aligned}
 A_2(i) &= - \left[\frac{\Delta t}{2(\Delta y^*)^2 \sqrt{P_r R_a}} + \frac{\Delta t}{4\Delta y^*} \nu_{i,j,n}^* \right], \\
 B_2(i) &= \left(1 + \frac{\Delta t}{(\Delta y^*)^2 \sqrt{P_r R_a}} + \frac{8F_s \beta_0 R_e \omega^* \Delta t}{\sqrt{P_r R_a}} \right), \\
 C_2(i) &= - \left(\frac{\Delta t}{2(\Delta y^*)^2 \sqrt{P_r R_a}} - \frac{\Delta t}{4\Delta y^*} \nu_{i,j,n}^* \right),
 \end{aligned}$$

$$\begin{aligned}
 D_2(i) = & \left(\frac{\Delta t}{2(\Delta x^*)^2 \sqrt{Pr Ra}} + \frac{\Delta t}{4\Delta x^*} v_{i,j,n}^* \right) \vartheta_{i-1,j}^* \\
 & + \left(1 - \frac{\Delta t}{(\Delta x^*)^2 \sqrt{Pr Ra}} \right) \vartheta_{i,j}^* + \frac{16F_s \beta_0 R_e \omega^* \Delta t}{\sqrt{Pr Ra}} \\
 & + \left(\frac{\Delta t}{2(\Delta x^*)^2 \sqrt{Pr Ra}} - \frac{\Delta t}{4\Delta x^*} v_{i,j,n}^* \right) \vartheta_{i+1,j}^* + \frac{\Delta t}{2} \phi.
 \end{aligned}$$

4.2 Equation of motion

$$\begin{aligned}
 \frac{\varepsilon_{i,j}^* - \varepsilon_{i,j,n}}{\frac{\Delta t}{2}} = & \sqrt{\frac{Pr}{Ra}} \left(\frac{\varepsilon_{i+1,j}^* - 2\varepsilon_{i,j}^* + \varepsilon_{i-1,j}^*}{(\Delta x^*)^2} + \frac{\varepsilon_{i,j+1,n} - 2\varepsilon_{i,j,n} + \varepsilon_{i,j-1,n}}{(\Delta y^*)^2} \right) \\
 (19) \quad & + (Ha)^2 \sqrt{\frac{Pr}{Ra}} \varepsilon_{i,j,n}
 \end{aligned}$$

$$\begin{aligned}
 \frac{\varepsilon_{i,j,n+1} - \varepsilon_{i,j}^*}{\frac{\Delta t}{2}} = & \sqrt{\frac{Pr}{Ra}} \left(\frac{\varepsilon_{i+1,j}^* - 2\varepsilon_{i,j}^* + \varepsilon_{i-1,j}^*}{(\Delta x^*)^2} + \frac{\varepsilon_{i,j+1,n+1} - 2\varepsilon_{i,j,n+1} + \varepsilon_{i,j-1,n+1}}{(\Delta y^*)^2} \right) \\
 (20) \quad & + (Ha)^2 \sqrt{\frac{Pr}{Ra}} \varepsilon_{i,j,n+1}
 \end{aligned}$$

Under boundary conditions,

$$\begin{aligned}
 (21) \quad v^* &= cons. & v_{0,j,n}^* &= 0, & v_{i,0,n}^* &= 0 \\
 \nu^* &= cons. & \nu_{0,j,n}^* &= 0, & \nu_{i,0,n}^* &= 0
 \end{aligned}$$

Equations (19) and (20) can be reduced in order to give,

$$(22) \quad A_3(i) \varepsilon_{i-1,j}^* + B_3(i) \varepsilon_{i,j}^* - C_3(i) \varepsilon_{i+1,j}^* = D_3(i),,$$

where

$$\begin{aligned}
 A_3(i) &= - \left(\frac{\Delta t}{2(\Delta x^*)^2} \sqrt{\frac{Pr}{Ra}} \right), \\
 B_3(i) &= \left(1 + \frac{\Delta t}{(\Delta x^*)^2} \sqrt{\frac{Pr}{Ra}} \right), \\
 C_3(i) &= - \left(\frac{\Delta t}{2(\Delta x^*)^2} \sqrt{\frac{Pr}{Ra}} \right), \\
 D_3(i) &= \left(\frac{\Delta t}{2(\Delta x^*)^2} \sqrt{\frac{Pr}{Ra}} \right) \varepsilon_{i,j-1,n} + \frac{\Delta t}{2(\Delta x^*)^2} \sqrt{\frac{Pr}{Ra}} \varepsilon_{i,j+1,n} \\
 &+ \left(1 - \frac{\Delta t}{(\Delta x^*)^2} \sqrt{\frac{Pr}{Ra}} + \frac{\Delta t (Ha)^2}{2} \sqrt{\frac{Pr}{Ra}} \right) \varepsilon_{i,j,n}.
 \end{aligned}$$

Followed,

$$(23) \quad A_4(i)\varepsilon_{i,j-1,n+1} + B_4(i)\varepsilon_{i,j,n+1} + C_4(i)\varepsilon_{i,j+1,n+1} = D_4(i)$$

where

$$\begin{aligned} A_4(i) &= - \left(\frac{\Delta t}{2(\Delta x^*)^2} \sqrt{\frac{P_r}{R_a}} \right), \\ B_4(i) &= \left(1 + \frac{\Delta t}{(\Delta x^*)^2} \sqrt{\frac{P_r}{R_a}} - \frac{\Delta t(H_a)^2}{2} \sqrt{\frac{P_r}{R_a}} \right), \\ C_4(i) &= - \left(\frac{\Delta t}{2(\Delta x^*)^2} \sqrt{\frac{P_r}{R_a}} \right), D_4(i) = \left(\frac{\Delta t}{2(\Delta x^*)^2} \sqrt{\frac{P_r}{R_a}} \right) \varepsilon_{i-1,j}^* \\ &+ \left(1 - \frac{\Delta t}{(\Delta x^*)^2} \sqrt{\frac{P_r}{R_a}} \right) \varepsilon_{i,j}^* + \frac{\Delta t}{2(\Delta x^*)^2} \sqrt{\frac{P_r}{R_a}} \varepsilon_{i+1,j}^*. \end{aligned}$$

The coefficients v^*, ν^* are treated as constants during any one time-step of the calculation [4], each of the equations (heat, motion) producing a tridiagonal system that is solved by the Gauss elimination process, all details are given in reference no. [18].

5. Results and data

In this section, we present some of the results obtained from the calculation carried out, and these results have been expressed by figures to explain how the solution for various cases becomes, as well as the effects of different parameters as follows figures:

6. Conclusions

In this work, we have used the ADI method in the solution of the governing equations completely without reducing or modifying, and from the results obtained we conclude that the steady-state can be reached after some iterations for all equations and this is clear from the figures given in the previous section, and the most important thing that has been achieved is the ADI method:

1. The higher the time stage, the further away from stability, as seen in the two Figures 2, 10.
2. The temperature within the boundary layer increases as the Brinkman number F_s increases. This is shown in Figure 4.
3. The temperature within the boundary layer decreases as the Boltzmann number β_0 increases. This is shown in Figure 5.

4. The temperature within the boundary layer increases as the amount of Reynolds number R_e increases. This is shown in Figure 6.
5. Figures 7, 12 shows that the effect of Rayleigh number R_a is constant in energy equation and motion, the higher the number of Rayleigh, the closer to equilibrium.
6. The effect of Prandtl number P_r on the equation energy was different from its effect on the equation of motion, as the more in the energy equation the further we moved away from stability, while we approached stability in the equation of motion by increasing the number as shown in Figures 8, 11.
7. The increase in Eckert number E_c is balanced by an increase in stability as shown in Fig. 9.
8. By reducing the Hartman number H_a , he offsets his stability convergence as shown in Fig.(13).

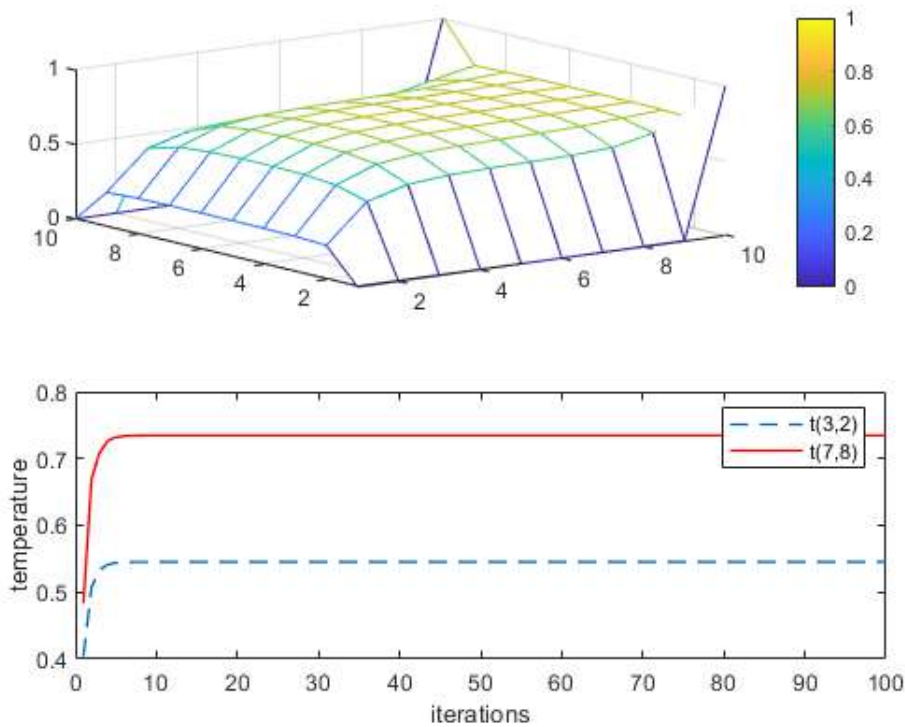


Figure 2: Temperature conduct

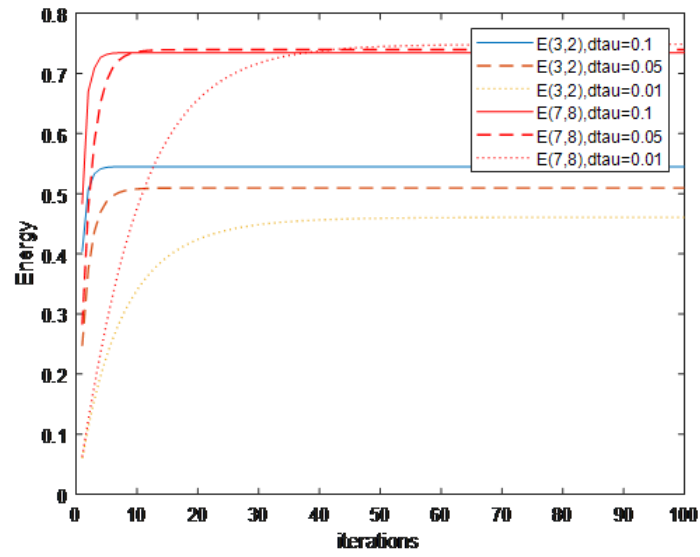
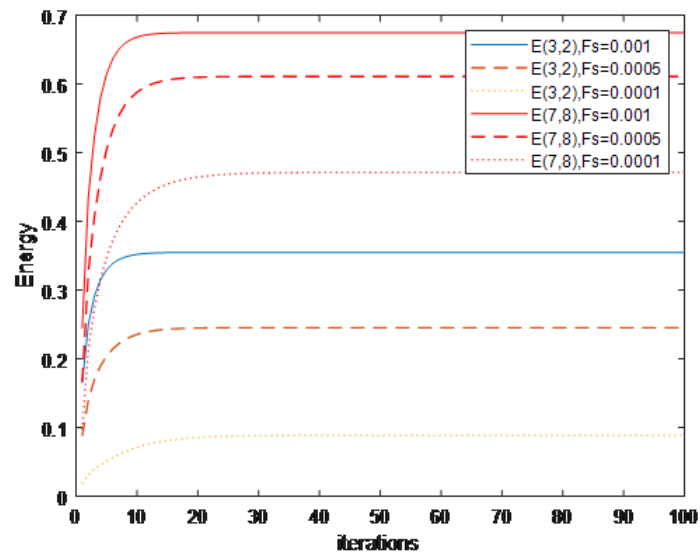


Figure 3: Impact of time-step on energy equation

Figure 4: Effect on the energy equation of Brinkman number F_s

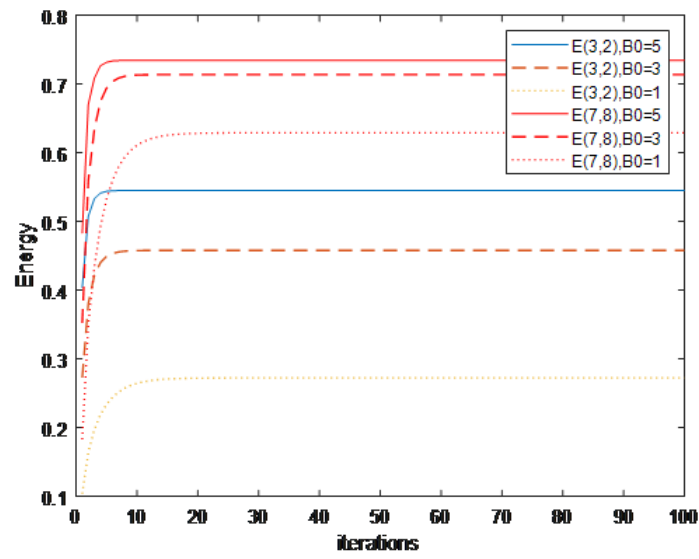


Figure 5: Effect on the energy equation of Boltzmann number B_0

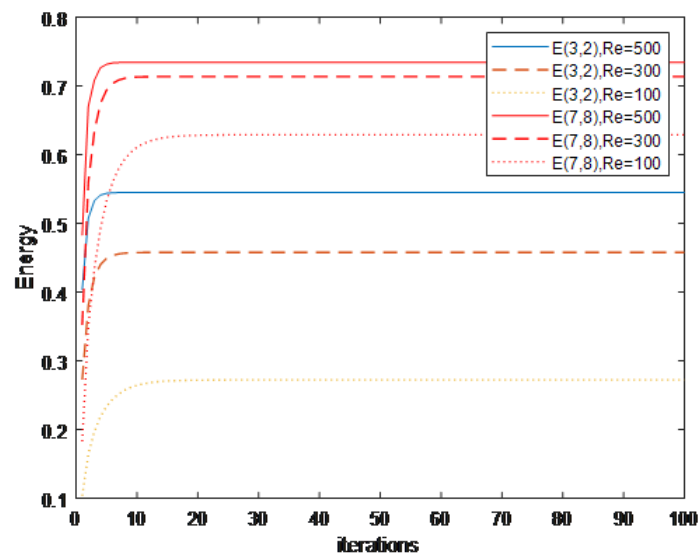


Figure 6: Effect of Reynolds number R_e in the energy equation

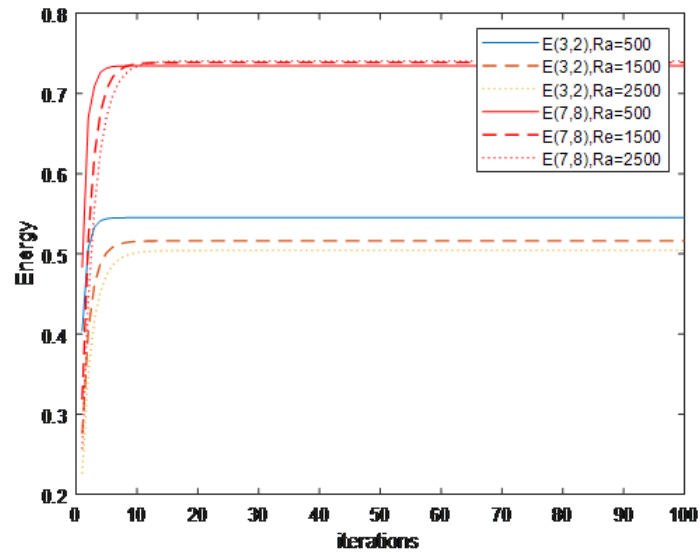


Figure 7: Effect of Rayleigh number R_a in energy equation number

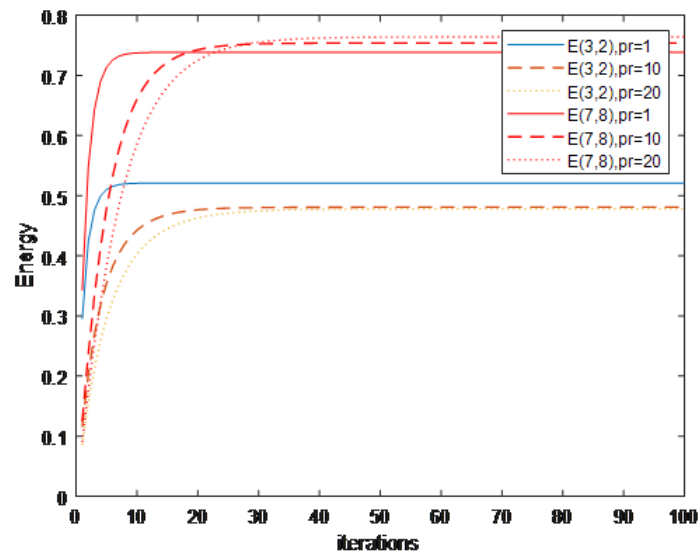


Figure 8: The impact of Prandtl number P_r on energy equations

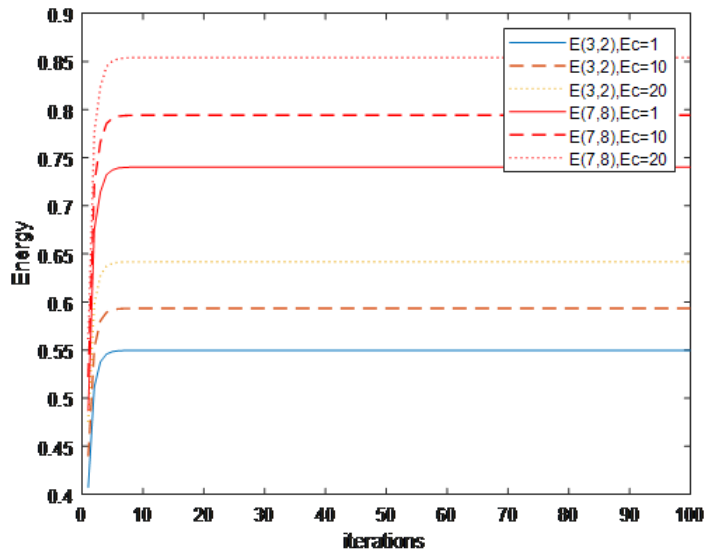


Figure 9: Impact of Eckert number E_c on energy equation

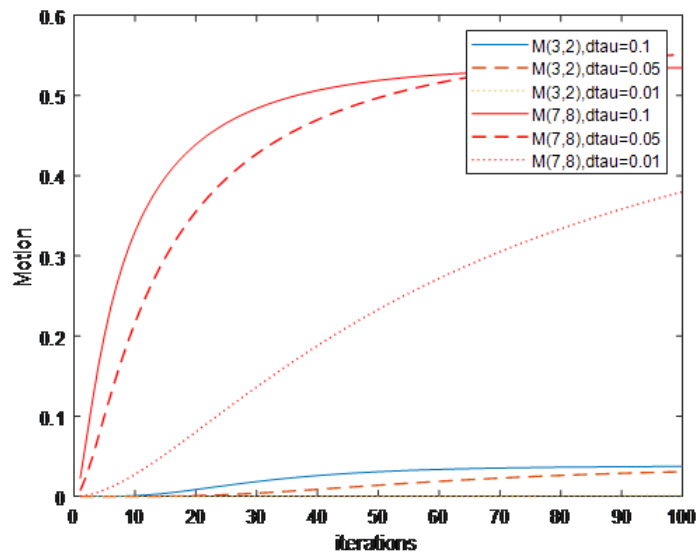


Figure 10: Time effect-step ($dtua$) on the motion equation

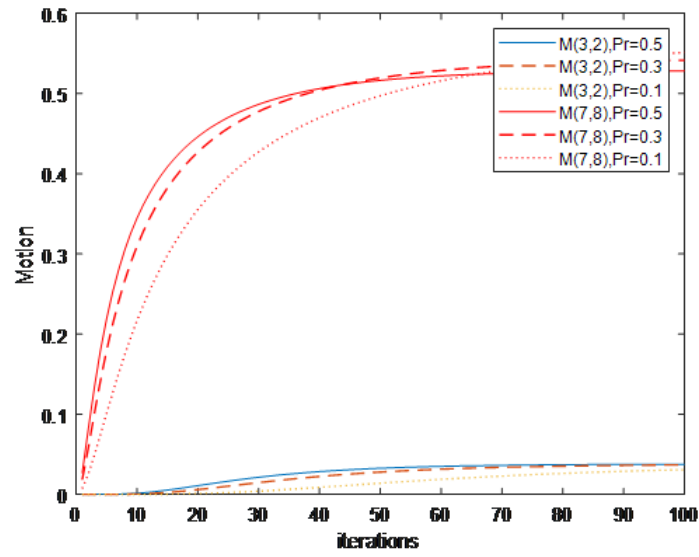


Figure 11: Influence of the Prandtl number P_r on the motion equation

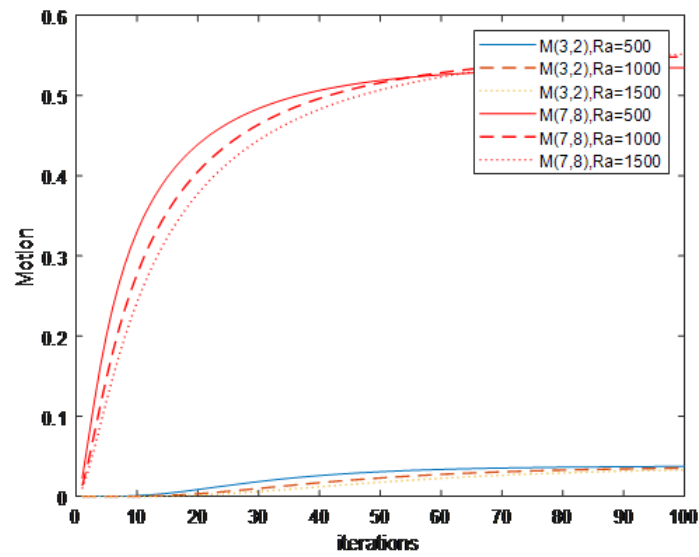


Figure 12: Effect of Rayleigh R_a number on motion equation

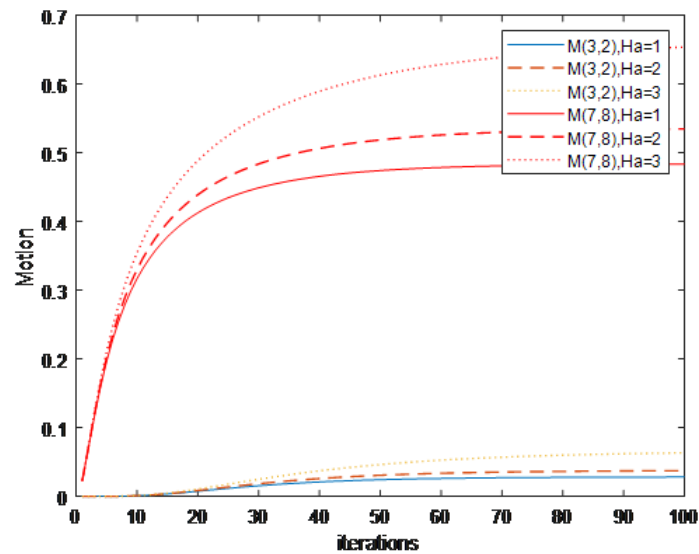


Figure 13: Effect of Hartman number H_a on motion equation

Acknowledgment

The authors are very thankful to the University of Mosul, College of Pure Science Education for its facilities, which have helped to enhance the quality of this work.

References

- [1] Z. Almishlih, A. Hammodat, *Numerical solution of fluid flow in horizontal tube under effects of radiation field*, Open Access Library Journal,7(2020), 1-12.
- [2] A. Bukhari, *Double diffusive convection in a horizontal porous layer superposed by a fluid layer*, Umm Al-Qura Univ. J. Sci. Med. Eng., 15 (2003), 95-113.
- [3] F.H. Busse, R.M. Clever, *Three dimensional convection in the presence of strong vertical magnetic field*, Eur. J. Mech. B. Fluids, 15 (1996), 1-15.
- [4] B. Carnhan, H. Luther, O. James, *Applied numerical methods*, John Wiely and Sons, INC. New York, London. Sydney.Toronto(1969).
- [5] P.G. Daniess, C.F. Ong, *A linear stability of convection in a rigid cannal uniformly heated from below*, Int. J. Heated and Mass Transfer, 33 (1990), 55-60.
- [6] A. Hammodat, T. Hamdoon, *Stability analysis of a fluid in a horizontal and oblique glass cavities*, Raf. J. of Comp. Sci. and Math., 11 (2014), 89-97.

- [7] J. Hartmann, F.H. Busse, *A convection in a rotating cylindrical annulus*, 350, 4 (1997), 209-229.
- [8] T. Hayat, R. Sajjad, Z. Abbas, M. Sajid, A.A. Hendi, *Radiation effects on MHD flow of Maxwell fluid in a channel with porous medium*, Int. J. of Heat and Mass Transfer, 54 (2011), 854-862.
- [9] W.F. Hughes, T.A. Brighten, *Schaum's outline of theory and problems of fluid dynamics*, McGraw-Hill Book Company, 1967.
- [10] K. Kumari, M. Goyal, *Heat and mass transfer flow of MHD viscous dissipative fluid in a channel with a stretching and porous plate*, An International Journal of Applied Mathematics and Information Sciences Letters, 5 (2017), 81-87.
- [11] T.R. Mahapatra, S.K. Nandy, A.S. Gupta, *Heat transfer in the magneto hydrodynamic flow of a power-law fluid past a porous flat plate with suction or blowing*, Int. Comm. In Heat and Mass Transfer, 39 (2012), 17-23.
- [12] M.S. Malashetty, J.C. Umavathi, J.P. Kumar, *Convection magneto hydrodynamic two fluid flow and heat transfer in an inclined channel*, J. Heat and Mass Transfer, 37 (2001), 259-264.
- [13] P. Mohne, O. Makinde, *Heat transfer to MHD oscillatory flow in a channel filled with porous medium*, Rom. J. Phys., 50 (2005), 931-938.
- [14] M.F. Mosa, *Radiative effect in magneto-fluid dynamic channel flow*, Ph.D. Thesis, University of Bradford March, 1979.
- [15] S. Mukhopadhyay, I.C. Mandal, *Magneto hydrodynamic (MHD) mixed convection slip flow and heat transfer over a vertical porous plate*, Engineering Science and Technology an International Journal, 18 (2015), 98-105.
- [16] M. Perty, F.H. Busse, *Convection in a rotation cylindrical annulus in the presence of magnetic field*, Eru. J. Mech. B. Fluids, 16 (1977), 817-833.
- [17] K.G. Singha, *Analytical solution to the problem of MHD free convection of an electrically conducting fluid between two heated parallel plates in the presence of an induced magnetic field*, Int. J. of Applied Mathematics and Computation, 1 (2009), 183-193.
- [18] V. Soundalgekar, *Transient free convection flow of viscous dissipative fluid past a semi-infinite vertical plate*, J. of Applied Mechanics and Engineering, 4 (1999), 203-218.
- [19] Z. Tamour, U. Muhammad, A. Umair, T.M. Syed, *Homotopy analysis method for system of partial differential equations*, Int. J. of Modern Engineering Sciences, 1 (2012), 67-79.

- [20] K.E. Torrance, L. Orloff, *Experiments on natural convection in enclosures with localized heated from below*, J. Fluid Mech., 36 (1969), 21-31.
- [21] A. Umair, A. Farah, I. Ahmad, *Crank-Nicolson finite difference method for two-dimensional fractional sub-diffusion equation*, Journal of Interpolation and Approximation in Scientific Computing, 2 (2017), 18-29.
- [22] A. Umair, A. Farah, T. Syed, *Modified implicit fractional difference scheme for 2D modified anomalous fractional sub-diffusion equation*, Advances in Difference Equations, 185, DOI 10.1186/s13662-017-1192-4, 2017.
- [23] Howard B. Wilson, Louis H. Turcotte, David Halpern, *Advanced mathematics and mechanics applications using MATLAB*, 3rd Ed., Chapman and Hall/CRC, USA, 2003.
- [24] Y. Yang, *Natural convection flow and heat transfer in vertical and inclined glazing cavities*, M.Sc. Thesis, University of Massachusetts, 2003.

Accepted: December 01, 2021